

STATISTICAL INFERENCE ON LATENT SPACE MODELS FOR NETWORK DATA

BY JINMING LI^a, GONGJUN XU^b, AND JI ZHU^c

Department of Statistics, University of Michigan, Ann Arbor
^alijinmin@umich.edu; ^bgongjun@umich.edu; ^cjizhu@umich.edu

Latent space models are powerful statistical tools for modeling and understanding network data. While the importance of accounting for uncertainty in network analysis has been well recognized, the current literature predominantly focuses on point estimation and prediction, leaving the statistical inference of latent space models an open question. This work aims to fill this gap by providing a general framework to analyze the theoretical properties of the maximum likelihood estimators. In particular, we establish the uniform consistency and asymptotic distribution results for the latent space models under different edge types and link functions. Furthermore, the proposed framework enables us to generalize our results to the dependent-edge and sparse scenarios. Our theories are supported by simulation studies and have the potential to be applied in downstream inferences, such as link prediction and network testing problems.

1. Introduction. Network data have become increasingly prevalent in various fields of study and applications, such as social networks [Traud et al., 2012], biological networks [Bullmore and Sporns, 2009], trading networks [Chaney, 2014], and collaboration networks [Ji and Jin, 2016], among others. Such data consist of a collection of nodes, representing entities, and edges, representing the relationships or interactions between these entities. A network can be parameterized as an $n \times n$ adjacency matrix A , where n is the number of nodes and A_{ij} represents the information of the edge between nodes i and j , which can take various values depending on the specific applications. For example, in a friendship network on social media, A_{ij} may be binary, where $A_{ij} = 1$ if and only if two nodes are mutual friends; in neuroimaging networks, A_{ij} may represent transformed brain connectivity measures and take continuous values. In this paper, we consider the general setting where networks are undirected and have no self-loops, i.e., $A_{ij} = A_{ji}$ for all $1 \leq i < j \leq n$ and $A_{ii} = 0$ for all $1 \leq i \leq n$.

Latent space models are powerful tools to perform statistical modeling and inference on network data [Hoff et al., 2002, Smith et al., 2019, Athreya et al., 2017]. By embedding nodes in a lower-dimensional latent space, these models are able to not only capture the dependency of edges but also reveal the complex and heterogeneous network structure via the geometric relationships between the embedded positions in the latent space. One popular class of models is the inner product latent space model [Ma et al., 2020, Wang and Guo, 2023, Zhao et al., 2012, Young and Scheinerman, 2007, Eavani et al., 2015], which utilizes the inner product to measure the similarity of latent positions, characterizing important network properties, such as transitivity, assortativity, and community structure prevailed in social networks [Smith et al., 2019], or block and crossing patterns observed in neuroimaging networks [Amico and Goñi, 2018].

Many popular network latent space models fall into the following formulation. Let each node i be assigned with a latent position $z_i \in \mathbb{R}^r$ in the r -dimensional latent space and a

Keywords and phrases: latent space models, maximum likelihood inference, network analysis.

degree parameter $\alpha_i \in \mathbb{R}$ that accounts for node heterogeneity. Then for each node pair $1 \leq i < j \leq n$, we assume

$$(1) \quad A_{ij} \sim p(\cdot \mid \theta_{ij}) \text{ with } \theta_{ij} = \sigma(z_i^T z_j + \alpha_i + \alpha_j),$$

where each edge A_{ij} is a random variable following the distribution $p(\cdot \mid \theta_{ij})$ with the parameter θ_{ij} determined by the latent positions (z_i, z_j) and degree parameters (α_i, α_j) through a link function $\sigma(\cdot)$. Typically, $\sigma(\cdot)$ is a smooth and increasing function, ensuring that the model exhibits the desirable property that higher inner product similarity of latent positions and greater node heterogeneity values lead to higher expected values of A_{ij} . Examples of popular models that can be formulated as Equation (1) include:

- The Random Dot Product Graph (RDPG) model [Young and Scheinerman, 2007], which considers a linear model for binary networks: $A_{ij} \stackrel{i.i.d.}{\sim} \text{Bernoulli}(\theta_{ij})$ with $\sigma(x) = x$ and $\alpha = 0_{n \times 1}$. RDPG covers some popular discrete network latent space models, such as the positive definite Stochastic Block Model and its variants [Holland et al., 1983, Zhao et al., 2012].
- The universal inner product model [Ma et al., 2020], which incorporates the logistic link function for binary networks: $A_{ij} \stackrel{i.i.d.}{\sim} \text{Bernoulli}(\theta_{ij})$ with $\sigma(x) = 1/(1 + \exp^{-x})$. This model extends the inner product model proposed in Hoff et al. [2002] by introducing the node heterogeneity parameters $(\alpha_i, i = 1, \dots, n)$.
- The linear low-rank decomposition type models [Wang and Guo, 2023, Sun and Li, 2017], which aim to model Gaussian edges such as fMRI networks: $A_{ij} \stackrel{i.i.d.}{\sim} \mathcal{N}(\theta_{ij}, \delta^2)$ with variance δ^2 , $\sigma(x) = x$ and $\alpha = 0_{n \times 1}$.

While latent space models have been widely used for modeling network data, the important yet challenging statistical inference question remains unaddressed. This is not only crucial for quantifying the estimation uncertainty of latent positions, but can also facilitate downstream inference problems, such as link prediction and network testing. In the existing literature, the asymptotic distribution is only studied for the spectral embedding estimators under the RDPG model [Athreya et al., 2017]. However, RDPG, which models binary edges through a linear model, may not be the most suitable choice. Ma et al. [2020] models binary edges with a logistic link function and establishes average consistency result of latent positions. However, deriving asymptotic distribution results for latent positions under the logistic link setting, or other link functions and edge types in general, remain a challenging problem due to the non-linearity structures. The analysis techniques developed in the RDPG literature largely rely on the linear model structure and the corresponding spectral decomposition, which are not applicable to general settings with different edge types and link functions. Moreover, the properties of latent position estimators, under more realistic settings such as edge dependency and sparsity, have yet to be investigated.

In this work, we aim to establish statistical inference results for the maximum likelihood estimators of a general class of network latent space models. Our main contributions are summarized as follows.

1. We propose a unified and flexible framework for analyzing the theoretical properties of the maximum likelihood estimators of network latent space models under a general model setup. Our approach is based on the examination of the high-dimensional structures of the score vector and the Hessian matrix of the log-likelihood function, which is fundamentally different from the techniques used in the existing literature [e.g. Athreya et al., 2017, Ma et al., 2020]. To overcome the theoretical challenge arising from the singularity of the Hessian matrix due to the identifiability issue, we introduce a Lagrange-type adjustment to the likelihood function to accommodate the identifiability constraints, which allows for

the development of a comprehensive statistical inference framework for various network data settings.

2. To the best of our knowledge, this work is the first to establish the uniform consistency as well as asymptotic distribution results for the maximum likelihood estimators, not only for the binary edges with non-linear link function but also under general edge types and link functions. Notably, we show that the asymptotic variance is optimal in the sense of achieving the Cramer-Rao information lower bound. The established asymptotic distribution results would also pave the way for diverse downstream inference procedures in various network data applications, such as constructing confidence intervals for link predictions.
3. Adopting the same analysis framework, we further extend our results towards more practical settings, where the network is allowed to be sparse and edge variables are allowed to have additional dependencies beyond those explained by the latent positions.

The rest of this paper is organized as follows. We start by discussing the network model setting with independent edges in Section 2, where we present the problem setup and assumptions, the analysis techniques, and the main theoretical results. In Section 3, we extend the analysis towards the dependent-edge and sparse-edge settings. Comprehensive simulation results are presented in Section 4, and a data application involving a statistician coauthorship network is presented in Section 5. Additional numerical results and proofs are presented in the Supplementary Material.

2. Maximum Likelihood Inference via the Lagrange-Adjusted Hessian.

2.1. Problem Setup. Our goal is to analyze the properties of the maximum likelihood estimators of the general latent space model introduced in Equation (1), where the parameters of interests are $z_i \in \mathbb{R}^r$ and $\alpha_i \in \mathbb{R}$ for $1 \leq i \leq n$. Following the latent space model literature [Ma et al., 2020], we treat z_i and α_i as fixed parameters and do not pose specific distributional assumptions on how they are generated. For situations where these parameters are treated as latent random variables, our analysis could be regarded as making statistical inferences on the realized values of those latent variables.

We use the following notations throughout the analysis. Let $Z_{n \times r}$ represent the latent position matrix, with the i -th row z_i^T being the latent position vector for node i . Similarly, let $H_{n \times (r+1)}$ be a matrix with the i -th row defined as $h_i^T = (z_i^T, 1)$. Let $\alpha_{n \times 1}$ be the vector of node heterogeneity parameters. Denote ϕ as an $n(r+1)$ -dimensional vector, whose i -th block $\phi_i = (z_i^T, \alpha_i)^T$ is the $(r+1)$ -dimensional vector that includes all latent parameters associated with node i . Denote $\pi_{ij} = z_i^T z_j + \alpha_i + \alpha_j$ such that we can write $\theta_{ij} = \sigma(\pi_{ij})$, and in matrix form, denote $\Pi_{n \times n} = ZZ^T + \alpha 1_n^T + 1_n \alpha^T$, where 1_n is the n -dimensional vector with all entries being 1. Similarly, we use 0_n to denote the n -dimensional zero vector.

For each edge A_{ij} , $1 \leq i < j \leq n$, denote the log-likelihood function with respect to π_{ij} as

$$l(\pi_{ij}; A_{ij}) = \log p(A_{ij} | \theta_{ij}) = \log p(A_{ij} | \sigma(\pi_{ij})).$$

For simplicity, we write $l(\pi_{ij}; A_{ij})$ as $l(\pi_{ij})$ and further introduce $l'(\pi_{ij}), l''(\pi_{ij}), l'''(\pi_{ij})$ to denote the 1th, 2nd, 3rd-order derivatives of $l(\pi_{ij}; A_{ij})$ with regard to π_{ij} . Given $\Pi_{n \times n}$, if all the edges are independent, the log-likelihood function of the network data can be written as

$$L(\phi; A) = \sum_{i=1}^n \sum_{j=i+1}^n l(\pi_{ij}).$$

We use $\phi^*, \phi_i^*, z_i^*, \alpha_i^*, \pi_{ij}^*$, and θ_{ij}^* to denote the true parameters. We use $\|\cdot\|, \|\cdot\|_1, \|\cdot\|_F, \|\cdot\|_{\max}$ to denote matrix 2-norm, 1-norm, Frobenius norm, and max norm, correspondingly.

Following the literature [e.g. [Ma et al., 2020](#)], we consider the maximum likelihood estimators under boundedness constraints. Specifically, for some large constant M , we seek to maximize $L(\phi; A)$ subject to $\sup_{1 \leq i \leq n} \|\phi_i\| \leq M$. To address the identifiability issue of the model parameters, we impose additional constraints on the estimators such that Z is centered with $Z^T \mathbf{1}_n = 0_r$ and $Z^T Z/n$ is diagonal [[Zhang et al., 2022](#)]. Note that the diagonality assumption is mainly for analysis convenience, and for any other identifiability condition, our results still hold up to the corresponding transformation. We use $\hat{\phi}$, $\hat{\phi}_i$, \hat{z}_i , $\hat{\alpha}_i$, $\hat{\pi}_{ij}$, and $\hat{\theta}_{ij}$ to denote the corresponding maximum likelihood estimators that maximize $L(\phi; A)$ under the boundedness and identifiability constraints.

2.2. Assumptions. For the purpose of theoretical analysis, we make the following assumptions.

- I. All edge variables A_{ij} , $1 \leq i < j \leq n$, are independent conditioning on ϕ^* .
- II. There exists a large $M > 0$ such that the parameter set $\Xi = \{\phi \mid \sup_{1 \leq i \leq n} \|\phi_i\| \leq M\}$ contains the true parameters ϕ^* .
- III. There exists a positive definite $r \times r$ matrix Σ_Z such that $Z^{*T} Z^*/n \rightarrow \Sigma_Z$ as $n \rightarrow \infty$.
- IV. Z^* is centered such that $Z^{*T} \mathbf{1}_n = 0_r$ and the limiting covariance matrix Σ_Z is diagonal with unique eigenvalues.
- V. $l'''(\cdot)$ exists within Ξ . Furthermore, there exists $0 < b_L < b_U$ such that $b_L \leq -l''(\cdot) \leq b_U$ and $|l'''(\cdot)| \leq b_U$ within Ξ .
- VI. There exist $t > 0$ and $s > 0$ such that for all $x \geq 0$, $P(|l'_{ij}| > x) \leq \exp(-(x/t)^s)$.
- VII. For any $1 \leq i \leq n$, there exists Σ_i such that $-n^{-1} \sum_{j:j \neq i} l''(\pi_{ij}^*) h_j^* h_j^{*T} \xrightarrow{p} \Sigma_i$. For an integer m and any m node indices $\mathcal{I} = (i_1, i_2, \dots, i_m)$, there exists $\Omega_{\mathcal{I}}$ such that $n^{-1/2} ([S(\phi^*)]_{i_1}, [S(\phi^*)]_{i_2}, \dots, [S(\phi^*)]_{i_m}) \rightarrow \mathcal{N}(0, \Omega_{\mathcal{I}})$, where $S(\phi^*) = \frac{\partial L}{\partial \phi}|_{\phi=\phi^*}$ is the score vector evaluated at the true parameters ϕ^* and $[S(\phi^*)]_i$ denotes the subvector of $S(\phi^*)$ corresponding to all latent parameters associated with node i , i.e., ϕ_i^* .

Assumption I is a common independence assumption made by the existing literature [[Ma et al., 2020](#), [Young and Scheinerman, 2007](#), [Hoff et al., 2002](#)]. Assumption II is on the boundedness of the true parameters for the purpose of theoretical analysis and also commonly assumed [[Ma et al., 2020](#)]. In Section 3, we will discuss how to relax these two assumptions. Assumption III poses regular conditions on the asymptotic behavior of the covariance structure of latent positions Z^* . Assumption IV poses necessary identifiability conditions that enable statistical inference: Z^* needs to be centered, as otherwise α^* is not identifiable, and the diagonality requirement of Σ_Z avoids the common orthogonal transformation issue of Z^* . As mentioned, the diagonality assumption is mainly for convenience and can be replaced by any other $r(r-1)/2$ rotation constraints for identifiability. Hence, our results do not rely on the assumption that columns of Z^* have to be linearly independent. Assumption V requires the link function $\sigma(\cdot)$ to be smooth and the loglikelihood function $l(\pi_{ij})$ is concave with respect to π_{ij} , which is satisfied by many widely used link functions such as logit, Poisson and linear links. Assumption VI ensures the tail density of edge variables decay exponentially and similar assumptions are often made in the literature [[Bai and Liao, 2013](#)]. Finally, Assumption VII is necessary for characterizing the asymptotic distributions of maximum likelihood estimator $\hat{\phi}_i$. In the special case of $m = 1$, Assumption VII becomes that under the true parameters, for any $1 \leq i \leq n$, there exists Ω_i such that $n^{-1/2} \sum_{j:j \neq i} l'(\pi_{ij}^*) h_j^* \rightarrow \mathcal{N}(0, \Omega_i)$, where similar assumptions are made in the factor analysis literature [[Bai, 2003](#), [Wang, 2022](#)]. This assumption is naturally justified for commonly used link functions by the standard central limit theorem arguments under mild conditions. Similar justifications can be made for the multivariate case with m nodes.

2.3. Theoretical Analysis via Lagrange-Adjusted Hessian. In this section, we illustrate the roadmap of our analysis on the properties of maximum likelihood estimators while leaving the detailed proofs in the supplementary material. Before we dive into the analysis, it is worthwhile to first understand the structure of the Hessian matrix of the log-likelihood function, $H(\phi) = \frac{\partial^2 L}{\partial \phi \partial \phi^T}$, as it plays the central role in our analysis. Following the block structure of ϕ , we can present the $n(r+1) \times n(r+1)$ Hessian matrix $H(\phi)$ as $n \times n$ matrix blocks with size $(r+1) \times (r+1)$, i.e., $[H(\phi)]_{ij} = \frac{\partial^2 L}{\partial \phi_i \partial \phi_j^T}$ for $1 \leq i, j \leq n$. We can further write $H(\phi)$ into two parts such that $H(\phi) = H_L(\phi) + J_L(\phi)$, where each $(r+1) \times (r+1)$ block is:

$$(2) \quad \begin{aligned} [H_L(\phi)]_{ii} &= \sum_{j:j \neq i} l''(\pi_{ij}) h_j h_j^T, \quad [J_L(\phi)]_{ii} = 0_{(r+1) \times (r+1)}, \quad 1 \leq i \leq n; \\ [H_L(\phi)]_{ij} &= l''(\pi_{ij}) h_j h_i^T, \quad [J_L(\phi)]_{ij} = l'(\pi_{ij}) \begin{pmatrix} I_r & 0_r \\ 0_r^T & 0 \end{pmatrix}, \quad 1 \leq i < j \leq n. \end{aligned}$$

Two observations can be made: (1) $J_L(\phi)$ is of smaller order compared to $H_L(\phi)$, as the score vector near true value is close to zero in probability; and (2) $H_L(\phi)$ is dominated by the diagonal blocks, which are all positive definite sub-matrices. For convenience, in the following, we use similar notations $[\cdot]_i$ and $[\cdot]_{ij}$ to denote the i -th block of a vector corresponding to ϕ_i and the (i, j) -th block of a matrix corresponding to (ϕ_i, ϕ_j) , as in Assumption VII and Equation (2), respectively.

To establish the asymptotic properties of the maximum likelihood estimators, our main idea is to utilize the first order condition:

$$(3) \quad 0 = S(\hat{\phi}) = S(\phi^*) + H(\phi^*) \times (\hat{\phi} - \phi^*) + R(\hat{\phi}, \phi^*),$$

where recall that $S(\phi) = \frac{\partial L}{\partial \phi}$ is the score vector and $H(\phi)$ is the Hessian matrix of the log-likelihood function, and $R(\hat{\phi}, \phi^*)$ denotes the residual term that depends on both $\hat{\phi}$ and ϕ^* . Ideally, we would want the following two conjectures hold: (1) the residual terms were uniformly a smaller order term and could be neglected; and (2) the Hessian matrix were negative definite after proper scaling. If both conjectures were true, we could show that for each $1 \leq i \leq n$,

$$\begin{aligned} \sqrt{n} (\hat{\phi}_i - \phi_i^*) &= -\sqrt{n} [H^{-1}(\phi^*) S(\phi^*)]_i + o_p(1) \\ &= [-n^{-1} H_L(\phi^*)]_{ii}^{-1} [n^{-1/2} S(\phi^*)]_i + o_p(1), \end{aligned}$$

where the last formula would allow us to establish the individual asymptotic distribution using the central limit theorem.

However, there are two major theoretical challenges in proving the conjectures above. For conjecture (1), establishing asymptotic distribution for every $1 \leq i \leq n$ require a uniform upper bound of $[R(\hat{\phi}, \phi^*)]_i$, which means we need to go beyond the average consistency of $\hat{\phi}$ and prove uniform consistency. We overcome this challenge by considering the integral form mean value theorem for vector-valued functions, which can be seen as a lower-order expansion of the first-order condition in Equation (3):

$$(4) \quad 0 = S(\hat{\phi}) = S(\phi^*) + \tilde{H} \times (\hat{\phi} - \phi^*),$$

where $\tilde{H} = \int_0^1 H(\phi^* + t(\hat{\phi} - \phi^*)) dt$. Thus, if we were able to show that the Hessian matrix is negative definite after proper rescaling, we could characterize the uniform norm of $\hat{\phi} - \phi^*$. Hence, the second and most critical challenge needs to be solved is to verify conjecture (2) within a small neighborhood of ϕ^* . Unfortunately, it turns out that the negative definite

statement is not true. As shown in the proofs in the supplementary material, the leading term of the Hessian matrix, $H_L(\phi^*)$, has exactly $r(r+1)/2$ eigenvalues equal to 0, which coincides with the number of constraints required for the model identifiability.

To address the challenges caused by singular Hessian matrices similar to what we have, the idea of introducing auxiliary Lagrange multiplier terms has been adopted in the literature of maximum likelihood inference. For example, [Silvey \[1959\]](#) and [Aitchison and Silvey \[1958\]](#) utilized the idea to study the constrained maximum likelihood inference problems with low-dimensional models. [El-Helbawy and Hassan \[1994\]](#) further explored the technique of using Lagrangian multiplier terms to study the likelihood functions with singular information matrices, while still limiting the discussion in the classic low-dimensional settings. Recently, [Wang \[2022\]](#) adopted a similar idea to analyze the maximum likelihood estimators of the high-dimensional factor analysis models. We want to emphasize that compared with the existing works, analyzing network latent space models has several unique challenges that are not trivial to overcome. For instance, the latent positions of network latent space models jointly appear as ZZ^T , which causes significantly more challenges in studying the structure of the Hessian matrix, especially the characterization of its matrix 1-norm. Moreover, due to the distinctive properties of network data, our analysis involves models with node heterogeneity parameters and considers the sparse network setting (see details in Section 3), which introduces additional challenges in theoretical analysis that the existing techniques do not fit directly.

Motivated by the existing literature, for theoretical analysis, we consider a modified loss function that combines the log-likelihood function with additional Lagrange-type penalty terms that correspond to the identifiability constraints of the network model. Formally, we consider the loss function below:

$$(5) \quad Q(\phi) = L(\phi) + P(\phi) := \sum_{i=1}^n \sum_{j=i+1}^n l(\pi_{ij}) - \frac{c}{2} n^2 \|\text{upper_diag}(Z^T Z/n)\|_F^2 - \frac{c}{2} n^2 \left\| \frac{Z^T \mathbf{1}_n}{n} \right\|_F^2,$$

where $L(\phi) = \sum_{i=1}^n \sum_{j=i+1}^n l(\pi_{ij})$ is the log-likelihood function, $P(\phi)$, which is defined as the last two terms in Equation (5), poses penalties on the off-diagonal entries of $Z^T Z/n$ as well as the mean vector of Z , and c is a multiplier satisfying $0 < c < b_L$, with b_L specified in Assumption V. The two penalty terms in $P(\phi)$ correspond to the rotation and centering identifiability conditions listed in Assumption IV. In the case where different rotation identifiability conditions are used, our analysis can be adapted accordingly by changing the first penalty term in $P(\phi)$.

We would like to highlight that the estimators of the model parameters, denoted by $\hat{\phi}$, obtained by maximizing $Q(\phi)$ are the corresponding maximum likelihood estimators introduced in Section 2.1 that satisfy the desired identifiability constraints. In particular, the task of maximizing Equation (5) is equivalent to the following two-step procedure: first obtaining a set of estimators of the model parameters from maximizing $L(\phi)$ only, and then transforming the obtained set of estimators (particularly \hat{Z}) such that they satisfy the considered identifiability conditions. This is because, due to the identifiability issue, within the equivalent class of all sets of “nonidentifiable” estimators, they all yield the same value of $L(\phi)$, while the identifiability constraints further refine them to the set of estimators corresponding to directly optimizing Equation (5). Therefore, the choice of the positive constant c does not affect the estimation, and practically, when calculating $\hat{\phi}$, we use the equivalent two-step procedure, which does not rely on c .

For the same reason, we further emphasize that the additional $P(\phi)$ in Equation (5) does not work the same way as the penalty terms in the literature of shrinkage regression, and similarly the parameter c does not function as a tuning parameter but rather a theoretical

tool for us to study the properties of the maximum likelihood estimators. In particular, in the theoretical analysis, it can be proved that the Hessian matrix of $P(\phi)$ can be written as $r(r+1)/2$ linearly independent vectors that form a basis of the null space of $H_L(\phi)$. Thus, the Hessian matrix of $Q(\phi)$ is negative definite with the information provided by $P(\phi)$ and all the analysis aforementioned can be applied to the maximizers of $Q(\phi)$, as they also satisfy the first order condition (Equation (3)).

With the proposed analysis techniques, we can establish the following theoretical results.

THEOREM 2.1 (Uniform and Average Consistency). *Under Assumptions I-VI, for any $\epsilon > 0$, we have*

$$\|\hat{\phi} - \phi^*\|_{max} = O_p(n^{-1/2+\epsilon}).$$

Moreover, under Assumptions I-VII, we have

$$\frac{1}{n}\|\hat{\phi} - \phi^*\|^2 = O_p\left(\frac{1}{n}\right).$$

REMARK 2.1. The uniform consistency rate established in Theorem 2.1 is nearly optimal, approaching the best rate of individual consistency $O_p(n^{-1/2})$. This result has not been established in the existing literature on network latent space models except under the RDGP model [Athreya et al., 2017]. However, the techniques used to analyze RDGP rely on the linear model structure, whereas our analytical framework is applicable to the general class of latent space models. As for average consistency, the rate established in Theorem 2.1 is optimal and aligns with the rate obtained in Ma et al. [2020], which focuses on binary networks with logistic link function and Bernoulli edges. However, our proof is different from Ma et al. [2020] and utilizes convexity arguments that not only suit broader settings but also lead to new results on the uniform consistency as well as asymptotic normality property as shown in the following theorem.

Next, we develop theories to enhance statistical inference involving either individual or multiple nodes, a topic scarcely explored in the existing literature. Given m node indices $\mathcal{I} = (i_1, i_2, \dots, i_m)$, denote the following consistent estimators of covariance matrices introduced in Assumption VII:

$$(6) \quad \begin{aligned} \hat{\Sigma}_{\mathcal{I}} &= \text{diag}(\hat{\Sigma}_{i_1}, \hat{\Sigma}_{i_2}, \dots, \hat{\Sigma}_{i_m}) \text{ with } \hat{\Sigma}_i = \frac{1}{n} \sum_{j:j \neq i} l''(\hat{\pi}_{ij}) \hat{h}_j \hat{h}_j^T, \quad i \in \mathcal{I}; \\ \hat{\Omega}_{\mathcal{I}} &= \left([\hat{\Omega}_{\mathcal{I}}]_{ij} \right) \text{ with } [\hat{\Omega}_{\mathcal{I}}]_{ij} = \frac{1}{n} \sum_{k_1:k_1 \neq i} \sum_{k_2:k_2 \neq j} l'(\hat{\pi}_{ik_1}) l'(\hat{\pi}_{jk_2}) \hat{h}_{k_1} \hat{h}_{k_2}^T, \quad i, j \in \mathcal{I}. \end{aligned}$$

THEOREM 2.2 (Joint Asymptotic Distribution). *Given m node indices $\mathcal{I} = (i_1, i_2, \dots, i_m)$, denote $\phi_{\mathcal{I}} = (\phi_{i_1}^T, \phi_{i_2}^T, \dots, \phi_{i_m}^T)^T$. Under Assumptions I-VII, we have*

$$\sqrt{n} \left[\widehat{\text{Var}}(\hat{\phi}_{\mathcal{I}}) \right]^{-1/2} (\hat{\phi}_{\mathcal{I}} - \phi_{\mathcal{I}}^*) \xrightarrow{d} \mathcal{N}(0, I_{m(r+1)}),$$

where $\widehat{\text{Var}}(\hat{\phi}_{\mathcal{I}}) = \hat{\Sigma}_{\mathcal{I}}^{-1} \hat{\Omega}_{\mathcal{I}} \hat{\Sigma}_{\mathcal{I}}^{-1}$ and $\hat{\Sigma}_{\mathcal{I}}$ together with $\hat{\Omega}_{\mathcal{I}}$ are defined in Equation (6).

In the special case of $m = 1$, we have the following individual asymptotic distribution result.

COROLLARY 2.2.1 (Individual Asymptotic Distribution). *Under Assumptions I-VII, for each $1 \leq i \leq n$,*

$$\sqrt{n} \left[\widehat{\text{Var}}(\hat{\phi}_i) \right]^{-1/2} (\hat{\phi}_i - \phi_i^*) \xrightarrow{d} \mathcal{N}(0, I_{r+1}),$$

where $\widehat{\text{Var}}(\hat{\phi}_i) = \hat{\Sigma}_i^{-1} \hat{\Omega}_i \hat{\Sigma}_i^{-1}$, with $\hat{\Sigma}_i$ defined in Equation (6) and $\hat{\Omega}_i = \frac{1}{n} \sum_{j:j \neq i} (l'(\hat{\pi}_{ij}))^2 \hat{h}_j \hat{h}_j^T$.

REMARK 2.2. The asymptotic distributions of maximum likelihood estimators derived in Theorem 2.2 and Corollary 2.2.1 are optimal in the sense of achieving the Cramer-Rao information lower bound. Under the RDGP model, our asymptotic variance also coincides with the result of the Adjacency Spectral Embedding estimator [Athreya et al., 2017]. Nevertheless, as discussed in Remark 2.1, our analysis adopts a different approach and our result holds for a more general class of network latent space models. Furthermore, the asymptotic variance can be estimated by samples, which allows for straightforward inference on ϕ_i such as constructing confidence regions.

The joint distribution result is useful for various downstream inference problems, such as link prediction inference, network testing problems, and network-assisted regression. For instance, for link prediction inference with Bernoulli edge variables and logistic link function, the following result can be naturally established by utilizing Theorem 2.2 for the special case of two nodes and Slutsky's theorem. Specifically, given $\mathcal{I} = \{i, j\}$, $1 \leq i < j \leq n$, under Assumptions I-VII, if A_{ij} are Bernoulli random variables and $\sigma(x) = 1/(1 + e^{-x})$, we have

$$(7) \quad \sqrt{n} \left[\widehat{\text{Var}}(\hat{\theta}_{ij}) \right]^{-1/2} (\hat{\theta}_{ij} - \theta_{ij}^*) \xrightarrow{d} \mathcal{N}(0, 1),$$

where in this case θ_{ij} is the linkage probability between node i and node j , and

$$\widehat{\text{Var}}(\hat{\theta}_{ij}) = \left[\hat{\theta}_{ij}(1 - \hat{\theta}_{ij}) \right]^2 \begin{pmatrix} \hat{h}_j \\ \hat{h}_i \end{pmatrix}^T \begin{pmatrix} \hat{\Sigma}_i^{-1} & 0 \\ 0 & \hat{\Sigma}_j^{-1} \end{pmatrix} \hat{\Omega}_{\mathcal{I}} \begin{pmatrix} \hat{\Sigma}_i^{-1} & 0 \\ 0 & \hat{\Sigma}_j^{-1} \end{pmatrix} \begin{pmatrix} \hat{h}_j \\ \hat{h}_i \end{pmatrix}.$$

3. Generalization towards Dependent-Edge and Sparse Settings. In this section, we further extend our analysis towards the dependent-edge and sparse network settings, which represent more realistic scenarios but also pose greater theoretical challenges. To the best of our knowledge, we are the first to establish the asymptotic properties of the maximum likelihood estimators under these settings.

3.1. Results for Dependent-Edge Networks. In the existing literature of network latent space models, a common assumption being made is that the latent positions are sufficient to account for the dependency structure among edges. Thus, edge variables A_{ij} are usually assumed to be conditionally independent as in Assumption I. However, this assumption in practice does not always hold for reasons such as mis-specifying the dimension of latent space. We therefore consider the setting where edge variables A_{ij} are allowed to have additional weak dependencies after conditioning on ϕ . Under these settings, the network latent space model can be seen as a proxy working model and the estimators are the maximizers of the pseudo-likelihood function. With the same analysis techniques on the Lagrange-adjusted Hessian, we demonstrate that theoretical results can still be established.

For the theoretical analysis, we relax Assumption I and substitute it with the following assumptions related to the boundedness of a few moment quantities. These assumptions restrict the edge dependencies from being overly strong, which could otherwise influence the validity of inference.

VIII. There exists $M > 0$ large enough such that

- i. $\frac{1}{n} \sum_{i=1}^n \sum_{j:j \neq i} \left[\frac{1}{n} \sum_{m=1}^n \mathbb{E}(l'(\pi_{mi}^*) l'(\pi_{mj}^*)) \right]^2 \leq M.$
- ii. $\mathbb{E} \left\{ \frac{1}{\sqrt{n}} \sum_{m=1}^n \left[l'(\pi_{mi}^*) l'(\pi_{mj}^*) - \mathbb{E}(l'(\pi_{mi}^*) l'(\pi_{mj}^*)) \right] \right\}^2 \leq M$ for all $1 \leq i < j \leq n.$
- iii. $\mathbb{E} \left\| \frac{1}{n^{3/4}} \sum_{i=1}^n \sum_{j:j \neq i} l''(\pi_{ij}^*) h_j^* h_i^{*T} \right\|^2 \leq M.$

IX. There exists $M > 0$ large enough and $\zeta > 2$ such that

$$\mathbb{E} \left(\frac{1}{n} \sum_{i=1}^n \left\| \frac{1}{\sqrt{n}} \sum_{j:j \neq i} l'(\pi_{ij}^*) h_j^* \right\|^\zeta \right) \leq M.$$

X. There exists $M > 0$ large enough such that for all $1 \leq s \leq n$:

- i. $\mathbb{E} \left\| \frac{1}{n} \sum_{i=1}^n \sum_{j:j \neq i} (n^{-1} \sum_{m=1}^n l''(\pi_{mj}^*) h_m^* h_m^{*T})^{-1} l'(\pi_{ij}^*) h_j^* h_i^{*T} l''(\pi_{is}^*) \right\|^2 \leq M.$
- ii. $\mathbb{E} \left\| \frac{1}{n} \sum_{i:i \neq s} \sum_{j:j \neq s} (n^{-1} \sum_{m=1}^n l''(\pi_{mi}^*) h_m^* h_m^{*T})^{-1} l'(\pi_{si}^*) l'(\pi_{sj}^*) h_j^* \right\|^2 \leq M.$

Assumptions VIII-X aim to characterize the strength of dependency among edge variables. Specifically, Assumptions VIII and IX restrict the dependent behavior of the score vector and Hessian matrix and are useful to establish uniform consistency results, whereas Assumption X limits the order of residual term, $R(\hat{\phi}, \phi^*)$, in Equation (3) and hence leads to the asymptotic distribution results under the edge-dependent setting.

Compared to the setup in Section 2.3, all three assumptions are satisfied when the edge variables are independent (Assumption I). These assumptions also hold when the edge variables are weakly correlated, such as introduced by decaying-product correlation structure or by additional sparse latent position dimension that is not estimated. In simulation studies, we consider specific dependent data settings to study the corresponding correlation settings aforementioned. We refer to Section 4 for more details.

We summarize the main theorems as follows.

THEOREM 3.1 (Uniform and Average Consistency). *Under Assumptions II-VI and VIII-IX, we have*

$$\|\hat{\phi} - \phi^*\|_{\max} = O_p(n^{-1/2+1/\zeta}).$$

Under Assumptions II-VIII, we have

$$\frac{1}{n} \|\hat{\phi} - \phi^*\|^2 = O_p\left(\frac{1}{n}\right).$$

REMARK 3.1. Compared to Theorem 2.1, the uniform consistency rate becomes $O_p(n^{-1/2+1/\zeta})$, which relies on ζ defined in Assumption IX. This indicates the rate now depends on both the specific form of the likelihood function and the level of edge dependency. On the other hand, The average consistency rate remains optimal and consistent with the result in Section 2.3.

THEOREM 3.2 (Joint Asymptotic Distribution). *Given m node indices $\mathcal{I} = (i_1, i_2, \dots, i_m)$, denote $\phi_{\mathcal{I}} = (\phi_{i_1}^T, \phi_{i_2}^T, \dots, \phi_{i_m}^T)^T$. Under Assumptions II-X, we have*

$$\sqrt{n} \left[\widehat{\text{Var}}(\hat{\phi}_{\mathcal{I}}) \right]^{-1/2} (\hat{\phi}_{\mathcal{I}} - \phi_{\mathcal{I}}^*) \xrightarrow{d} \mathcal{N}(0, I_{m(r+1)}),$$

where $\widehat{\text{Var}}(\hat{\phi}_{\mathcal{I}}) = \hat{\Sigma}_{\mathcal{I}}^{-1} \hat{\Omega}_{\mathcal{I}} \hat{\Sigma}_{\mathcal{I}}^{-1}$ and $\hat{\Sigma}_{\mathcal{I}}$ together with $\hat{\Omega}_{\mathcal{I}}$ are defined in Equation (6).

REMARK 3.2. The asymptotic distribution results are the same as those established in Section 2.3. Similarly to Corollaries 2.2.1 and Equation (7), the individual asymptotic distribution of every latent position estimator as well as the link prediction inference results hold under Assumptions II-X. Compared to existing literature, asymptotic distribution results have only been established under the RDPG model [Athreya et al., 2017] with the independent edge setting. On the other hand, our approach is more general and can be adapted to the dependent edge setting.

3.2. *Results for Sparse Networks.* In the previous analysis under Assumption II, we only consider the bounded parameter space for the true parameters. This limitation primarily arises from the difficulty in the theoretical analysis, where the objective function is shown to exhibit strict concavity locally near the true parameters. However, this assumption poses an inherent restriction on the sparsity or signal-to-noise ratio of network data, which may be impractical in certain applications. For example, many social networks and communication networks are observed to have sparsity properties, indicating that the edge density tends to decrease as n increases.

In this section, we illustrate how to relax Assumption II and conduct the theoretical analysis of the likelihood function within an unbounded parameter space. Our approach is to generalize the model setup in Equation (1) by introducing a sparsity parameter that controls the overall edge density and is allowed to be unbounded. This new parameter allows us to quantify the influence of network sparsity on the properties of the maximum likelihood estimators. By modifying the penalty terms $P(\phi)$ and changing the assumptions accordingly, we are able to utilize the same analysis techniques to derive meaningful inference results. However, it is crucial to note that these modifications are case-specific and may vary for different link functions and edge types. Consequently, we focus our analysis on the popular latent space model for binary networks, with the logistic link function, $\sigma(x) = \text{logistic}(x) = 1/(1 + \exp(-x))$, and Bernoulli edge variables. The extensions towards other link functions and edge types can be performed similarly; see Remark 3.4 for more discussion.

Specifically, we generalize the model in Equation (1) into Equation (8) below, where $\rho_n \in \mathbb{R}$ is the newly introduced sparsity parameter that is allowed to be unbounded while z_i and α_i remain bounded.

$$(8) \quad A_{ij} \sim \text{Bernoulli}(\theta_{ij}), \quad \theta_{ij} = \text{logistic}(z_i^T z_j + \alpha_i + \alpha_j + \rho_n),$$

Our theoretical analysis is conducted under the setting that the sparsity parameter ρ_n is given, similar to the setting considered in the sparse low-rank matrix completion literature [Cape et al., 2019]. The estimators of Z and α are defined similarly as in Section 2.1, that is, the corresponding maximum likelihood estimators under the boundedness and identifiability constraints for Z and α . We emphasize that introducing ρ_n serves solely the purpose of characterizing the effect of network sparsity on inference results and do not change our inference targets (Z and α). Similar to the treatment in Cape et al. [2019], ρ_n shall be seen as a known parameter to characterize the effect of sparsity, which the estimators' consistency rates would depend on.

To make the notations consistent with previous sections, we keep using π_{ij} to denote $z_i^T z_j + \alpha_i + \alpha_j$ and ϕ_i to denote $(z_i^T, \alpha_i)^T$. Note that all the parameters of interests, ϕ_i and π_{ij} , do not include ρ_n . By separating the sparsity effect from the formulation of θ_{ij} with a standalone sparsity parameter (ρ_n), it facilitates our theoretical analysis of the maximum likelihood estimators for Z and α as follows. In particular, we follow the theoretical framework introduced in Section 2.3. Writing out the objective function in Equation (5) in the same

way, our theoretical analysis will focus on the following loss function:

$$(9) \quad Q(\phi) = L(\phi) + P(\phi) = \sum_{i=1}^n \sum_{j=i+1}^n l(z_i^T z_j + \alpha_i + \alpha_j + \rho_n) - \frac{c_n}{2} n^2 \|\text{upper_diag}(Z^T Z/n)\|_F^2 - \frac{c_n}{2} n^2 \left\| \frac{Z^T 1_n}{n} \right\|_F^2,$$

where we write the multiplier c as c_n , as it will be chosen to depend on the network sparsity (ρ_n), whose rationale is explained as follows. For simplicity, we still denote the likelihood function as $l(\pi_{ij}) = l(z_i^T z_j + \alpha_i + \alpha_j + \rho_n)$ when there is no ambiguity. Specifically, to address the challenge of strict concavity of $l(\pi_{ij})$ in the unbounded parameter space, we examine the limiting relations of $l'(\pi_{ij})$, $l''(\pi_{ij})$, $l'''(\pi_{ij})$ and ρ_n , so that after proper scaling the analysis reduces back into a bounded parameter space. For the model in Equation (8), we have:

$$(10) \quad \begin{aligned} l'(\pi_{ij}) &= A_{ij} - \theta_{ij}, \\ l''(\pi_{ij}) &= -\frac{e^{\pi_{ij} + \rho_n}}{(1 + e^{\pi_{ij} + \rho_n})^2}, \\ l'''(\pi_{ij}) &= -\frac{e^{\pi_{ij} + \rho_n}(-1 + e^{\pi_{ij} + \rho_n})}{(1 + e^{\pi_{ij} + \rho_n})^3}. \end{aligned}$$

When $\rho_n \rightarrow -\infty$ and π_{ij} remains bounded, all $l'(\pi_{ij})$, $l''(\pi_{ij})$, $l'''(\pi_{ij})$ can be rescaled with $w_n := 1/e^{\rho_n}$ such that similar conditions stated in Assumption V are valid. Correspondingly, the scaling factor for the Hessian matrix will also become $(w_n n)^{-1}$ and the order of penalty term $P(\phi)$ in Equation (9) should multiply w_n . Thus in (9), we choose $c_n = c w_n$ with constant $0 < c < e^{-M}$, where M is specified in the following Assumption II*. Theoretical properties of the estimators are established in the following.

REMARK 3.3. In practice when ρ_n is unknown, our estimation approach is to first estimate Z and α using the same procedure as in the independent-edge case of Section 2 (with the identifiability constraints), and then estimate ρ_n as the mean of the estimated α in the first step and set the final estimator of α to be centered. Note that the centering for α is needed for identifiability consideration, since the mean of α_i 's and ρ_n cannot be distinguished when ρ_n is unknown. Empirical consistency results are presented in the simulation results under the ‘‘Sparse’’ setting in Section 4. As will be shown below in our theoretical results, constructing confidence regions or intervals does not directly require the estimation of ρ_n , and our numerical results show that the established theory remains valid in the considered sparse edge setting.

REMARK 3.4. Before presenting the theoretical results, we briefly discuss how similar modifications can be made for other link functions and edge types. The main idea is to introduce a proper scaling parameter for the log-likelihood function of the original model, $l(\pi_{ij})$, and modify the assumptions based on the analysis of the order of its derivatives. Take the Gaussian edge variable with identity function as an example, it is reasonable to introduce a multiplicative parameter and consider the model

$$A_{ij} \sim \mathcal{N}(\theta_{ij}, \delta^2), \quad \theta_{ij} = \rho_n \sigma(z_i^T z_j + \alpha_i + \alpha_j),$$

where ρ_n , in this case, controls the overall signal-to-noise ratio and is allowed to decrease to zero for modeling low signal-to-noise ratio data.

We make the following assumptions to analyze the model in Equation (8) under the sparse network setting.

I*. With $w_n = e^{\rho_n}$, we have $\lim_{n \rightarrow \infty} w_n = 0$. Furthermore, there exists $\epsilon > 0$ such that $w_n = \Theta(n^{-1/2+\epsilon})$, i.e., there exists $C > 0$ such that $w_n \geq Cn^{-1/2+\epsilon}$.

II*. There exists $M > 0$ such that the parameter space $\Xi = \{\phi | \sup_{1 \leq i \leq n} \|\phi_i\| \leq M\}$ contains the true parameters ϕ^* .

III*. There exists a positive definite $r \times r$ matrix Σ_Z such that $Z^{*T}Z^*/n \rightarrow \Sigma_Z$ as $n \rightarrow \infty$.

IV*. The limiting covariance matrix Σ_Z is diagonal with unique eigenvalues. Also, Z^* is centered such that $Z^{*T}1_n = 0_r$.

V*. For any $1 \leq i \leq n$, there exists Σ_i such that $-(w_n n)^{-1} \sum_{j:j \neq i} l''(\pi_{ij}^*) h_j^* h_j^{*T} \xrightarrow{p} \Sigma_i$. For an integer m and any m node indices $\mathcal{I} = (i_1, i_2, \dots, i_m)$, there exists $\Omega_{\mathcal{I}}$ such that $(w_n n)^{-1/2} ([S(\phi^*)]_{i_1}, [S(\phi^*)]_{i_2}, \dots, [S(\phi^*)]_{i_m}) \rightarrow \mathcal{N}(0, \Omega_{\mathcal{I}})$.

VI*. There exists $M > 0$ large enough such that

- i. $\frac{1}{n} \sum_{i=1}^n \sum_{j:j \neq i} \left[\frac{1}{w_n n} \sum_{m=1}^n \mathbb{E}(l'(\pi_{mi}^*) l'(\pi_{mj}^*)) \right]^2 \leq M$.
- ii. $\mathbb{E} \left\{ \frac{1}{w_n \sqrt{n}} \sum_{m=1}^n \left[l'(\pi_{mi}^*) l'(\pi_{mj}^*) - \mathbb{E}(l'(\pi_{mi}^*) l'(\pi_{mj}^*)) \right] \right\}^2 \leq M$ for all $1 \leq i < j \leq n$.
- iii. $\mathbb{E} \left\| \frac{1}{\sqrt{w_n n^{3/4}}} \sum_{i=1}^n \sum_{j:j \neq i} l''(\pi_{ij}^*) h_j^* h_i^{*T} \right\|^2 \leq M$.

VII*. There exists $M > 0$ large enough and $\zeta > 2$ such that

$$\mathbb{E} \left(\frac{1}{n} \sum_{i=1}^n \left\| \frac{1}{w_n \sqrt{n}} \sum_{j:j \neq i} l'(\pi_{ij}^*) h_j^* \right\|^\zeta \right) \leq M.$$

VIII*. There exists $M > 0$ large enough such that for all $1 \leq s \leq n$:

- i. $\mathbb{E} \left\| \frac{1}{w_n n} \sum_{i=1}^n \sum_{j:j \neq i} ((w_n n)^{-1} \sum_{m=1}^n l''(\pi_{mj}^*) h_m^* h_m^{*T})^{-1} l'(\pi_{ij}^*) h_j^* h_i^{*T} l''(\pi_{is}^*) \right\|^2 \leq M$.
- ii. $\mathbb{E} \left\| \frac{1}{w_n n} \sum_{i:i \neq s} \sum_{j:j \neq s} (n^{-1} \sum_{m=1}^n l''(\pi_{mi}^*) h_m^* h_m^{*T})^{-1} l'(\pi_{si}^*) l'(\pi_{sj}^*) h_j^* \right\|^2 \leq M$.

Our analysis for the sparse network setting is compatible with the dependent edge setting, where the orders of the quantities in Assumptions V*-VIII* are rescaled with w_n accordingly. Assumption I* requires the edge density of the network to be at least of order $n^{-1/2+\epsilon}$, such that the effective sample size $w_n n$ is greater than \sqrt{n} when allowing for dependency. Assumptions II*-V* are similar to the previous Assumptions II-IV and VII-X on model regularity, identifiability, and weak dependency. The previous Assumptions V-VI on the likelihood function are satisfied by the model in Equation (8), hence they are not needed.

REMARK 3.5. If Assumption I holds, i.e., all edge variables are conditionally independent, Assumption I* can be relaxed to allow the network sparsity to be as low as $\Omega(n^{-1} \log^\epsilon n)$. This minimal sparsity level aligns with existing literature [Athreya et al., 2017, Ma et al., 2020], which consider specific latent space models with identity and logistic link functions for binary edges.

Our theoretical results are summarized as follows.

THEOREM 3.3 (Uniform and Average Consistency). *Under Assumptions I*-IV* and VI*-VII*, we have*

$$\|\hat{\phi} - \phi^*\|_{\max} = O_p((w_n n)^{-1/2+1/\zeta}).$$

Under Assumptions I*-V* and VI*, we have

$$\frac{1}{n} \|\hat{\phi} - \phi^*\|^2 = O_p\left(\frac{1}{w_n n}\right).$$

REMARK 3.6. In the sparse network setting, the consistency rates of maximum likelihood estimators are related to the rate at which w_n approaches 0. Similar results have been reported in the literature on sparse low-rank matrix completion [Cape et al., 2019] with a signal-plus-noise linear structure. However, our analysis adopts different techniques that are general and compatible with the dependent edge setting and non-linear model setups.

Before presenting the results on statistical inference under the sparse edge setting, note that the consistent estimators of covariance matrices are similar but not the same as those presented in Equation (6). Given m node indices $\mathcal{I} = (i_1, i_2, \dots, i_m)$, the following consistent estimators are scaled with the sparsity parameter w_n :

$$(11) \quad \begin{aligned} \hat{\Sigma}_{\mathcal{I}} &= \text{diag}(\hat{\Sigma}_{i_1}, \hat{\Sigma}_{i_2}, \dots, \hat{\Sigma}_{i_m}), \text{ with } \hat{\Sigma}_i = \frac{1}{w_n n} \sum_{j:j \neq i} l''(\hat{\pi}_{ij}) \hat{h}_j \hat{h}_j^T, \quad i \in \mathcal{I}; \\ \hat{\Omega}_{\mathcal{I}} &= \left([\hat{\Omega}_{\mathcal{I}}]_{ij} \right), \text{ with } [\hat{\Omega}_{\mathcal{I}}]_{ij} = \frac{1}{w_n n} \sum_{k_1:k_1 \neq i} \sum_{k_2:k_2 \neq j} l'(\hat{\pi}_{ik_1}) l'(\hat{\pi}_{jk_2}) \hat{h}_{k_1} \hat{h}_{k_2}^T, \quad i, j \in \mathcal{I}. \end{aligned}$$

THEOREM 3.4 (Joint Asymptotic Distribution). Given m node indices $\mathcal{I} = (i_1, i_2, \dots, i_m)$, denote $\phi_{\mathcal{I}} = (\phi_{i_1}^T, \phi_{i_2}^T, \dots, \phi_{i_m}^T)^T$. Under Assumptions I*-VIII*, we have

$$\sqrt{w_n n} \left[\widehat{\text{Var}}(\hat{\phi}_{\mathcal{I}}) \right]^{-1/2} (\hat{\phi}_{\mathcal{I}} - \phi_{\mathcal{I}}^*) \xrightarrow{d} \mathcal{N}(0, I_{m(r+1)}),$$

where $\widehat{\text{Var}}(\hat{\phi}_{\mathcal{I}}) = \hat{\Sigma}_{\mathcal{I}}^{-1} \hat{\Omega}_{\mathcal{I}} \hat{\Sigma}_{\mathcal{I}}^{-1}$ and $\hat{\Sigma}_{\mathcal{I}}$ together with $\hat{\Omega}_{\mathcal{I}}$ are defined in (11).

COROLLARY 3.4.1 (Individual Asymptotic Distribution). Under Assumptions I*-VIII*, for each $1 \leq i \leq n$,

$$\sqrt{w_n n} \left[\widehat{\text{Var}}(\hat{\phi}_i) \right]^{-1/2} (\hat{\phi}_i - \phi_i^*) \xrightarrow{d} \mathcal{N}(0, I_{r+1}),$$

where $\widehat{\text{Var}}(\hat{\phi}_i) = \hat{\Sigma}_i^{-1} \hat{\Omega}_i \hat{\Sigma}_i^{-1}$, with $\hat{\Sigma}_i$ defined in (11) and $\hat{\Omega}_i = \frac{1}{w_n n} \sum_{j:j \neq i} (l'(\hat{\pi}_{ij}))^2 \hat{h}_j \hat{h}_j^T$.

Importantly, Theorem 3.4 and Corollary 3.4.1 imply that constructing confidence regions and confidence intervals based on $\hat{\phi}_{\mathcal{I}}$ and $\hat{\phi}_i$, respectively, does not require the estimation of ρ_n or equivalently w_n . This is because (1) the scaling factor of the asymptotic variance term and the normalization factor in limiting distribution are canceled out; (2) the asymptotic terms related to w_n or ρ_n in $l'(\pi_{ij})$ and $l''(\pi_{ij})$ are asymptotically canceled out.

Similar to Equation (7), we use the following example as an illustration for link prediction inference. Given $\mathcal{I} = \{i, j\}$, $1 \leq i < j \leq n$, under Assumptions I*-VIII*, if A_{ij} are Bernoulli random variables and $\sigma(x) = 1/(1 + e^{-x})$, we have

$$(12) \quad \sqrt{w_n n} \left[\widehat{\text{Var}}(\hat{\theta}_{ij}) \right]^{-1/2} (\hat{\theta}_{ij} - \theta_{ij}^*) \xrightarrow{d} \mathcal{N}(0, 1),$$

where in this case θ_{ij} is the linkage probability between node i and node j , and

$$\widehat{\text{Var}}(\hat{\theta}_{ij}) = \left[\hat{\theta}_{ij}(1 - \hat{\theta}_{ij}) \right]^2 \begin{pmatrix} \hat{h}_j \\ \hat{h}_i \end{pmatrix}^T \begin{pmatrix} \hat{\Sigma}_i^{-1} & 0 \\ 0 & \hat{\Sigma}_j^{-1} \end{pmatrix} \hat{\Omega}_{\mathcal{I}} \begin{pmatrix} \hat{\Sigma}_i^{-1} & 0 \\ 0 & \hat{\Sigma}_j^{-1} \end{pmatrix} \begin{pmatrix} \hat{h}_j \\ \hat{h}_i \end{pmatrix}.$$

Similar to Theorem 3.4 and Corollary 3.4.1, constructing confidence regions or intervals for θ_{ij} does not require estimating ρ_n . When constructing intervals in practice, one could further remove the w_n implicitly contained in θ_{ij}^* in the variance term with asymptotic approximations. However, through simulation studies, we find that constructing confidence intervals with the current form gives better coverage rates. This is potentially because removing w_n would cause finite-sample estimation bias.

4. Simulation Study.

4.1. Experiment Setup. In this section, we present experiment results on (1) evaluating consistency rates of the maximum likelihood estimators; (2) constructing confidence intervals for latent positions; and (3) constructing confidence intervals for link prediction probabilities. Here we focus on the latent space model for binary networks with link function $\sigma(x) = \text{logistic}(x) = 1/(1 + \exp(-x))$ and Bernoulli edge variables, as presented in Equation (8), under different simulation settings including independent edges with bounded parameter space, dependent edges, and sparse networks. Simulation results of similar experiments for the network latent space model with continuous Gaussian edge variables can be found in the supplementary material. Details of the data generating processes will be discussed in each setting below. For the estimation procedure, we adopt a singular value thresholding approach as in Algorithm 3 of Ma et al. [2020] and a projected gradient descent method as in Algorithm 1 of Ma et al. [2020] for initialization and optimization, respectively.

4.2. Independent Edges with Bounded Parameter Space. We first consider the independent setting as discussed in Section 2.3, referred as “Bounded & Indep.”. The network data is generated as follows. We set $r = 2$, generate i.i.d. entries of Z from a truncated normal distribution $\mathcal{N}_{[-2,2]}(0, 1)$ and i.i.d. entries of α from a uniform distribution $U([1, 3])$. To satisfy the identifiability conditions, we first center Z and α , and set $\rho_n = -3$. Under such data generating process, the average edge density of networks is around 0.08. The number of nodes n ranges from 500 to 8000, and for each n , we repeat the experiment 200 times by sampling i.i.d. networks from the same Z , α , and ρ_n .

For the consistency of maximum likelihood estimators, we evaluate $\Delta Z = \|Z - \hat{Z}\|_F^2/n^2$, $\Delta\alpha = \|\alpha - \hat{\alpha}\|^2/n^2$, $\Delta\rho_n = (\rho_n - \hat{\rho}_n)^2$, and $\Delta\text{Var}(\hat{z}_{11}) = (\text{Var}(\hat{z}_{11}) - \widehat{\text{Var}}(\hat{z}_{11}))^2$, where the last quantity is the measuring the estimation error of the plug-in estimator of the first coordinate of the first latent position (Equation (6)) and we estimate ρ_n as the mean of $\hat{\alpha}$. The results are illustrated in the log-log scaled plots on the first row of Figure 1. We can see the maximum likelihood estimators have consistency rates that meet theoretical results and both ρ_n and $\text{Var}(\hat{z}_{11})$ can be consistently estimated.

To evaluate the distributional results of latent positions, we focus on the first coordinate of the first latent position z_{11} for an illustration. Figure 2 plots the histograms of $z_{11} - \hat{z}_{11}$ together with the theoretical density curves, as well as the QQ-plots, where we can see that as n grows the empirical distribution is converging to the theoretical distribution. We further construct 95% confidence intervals for z_{11} and the linkage probability of node 1 and 2, i.e., $\theta_{1,2}$, according to Corollary 2.2.1 and Equation (7) with the plug-in variance estimators. The average coverage rates are reported in the first rows of Table 1 and Table 2, respectively, where we can see that the empirical coverage rates meet the expectation as n grows.

4.3. Dependent Edges. We consider two ways of introducing dependency between edges. In the first setting, referred as “Dependent-1”, we generate Z , α , and ρ_n with the same setting as Section 4.2. Then we use R package CorBin [Jiang et al., 2021] to generate dependent Bernoulli edge variables with the decaying-product correlation structure [Jiang

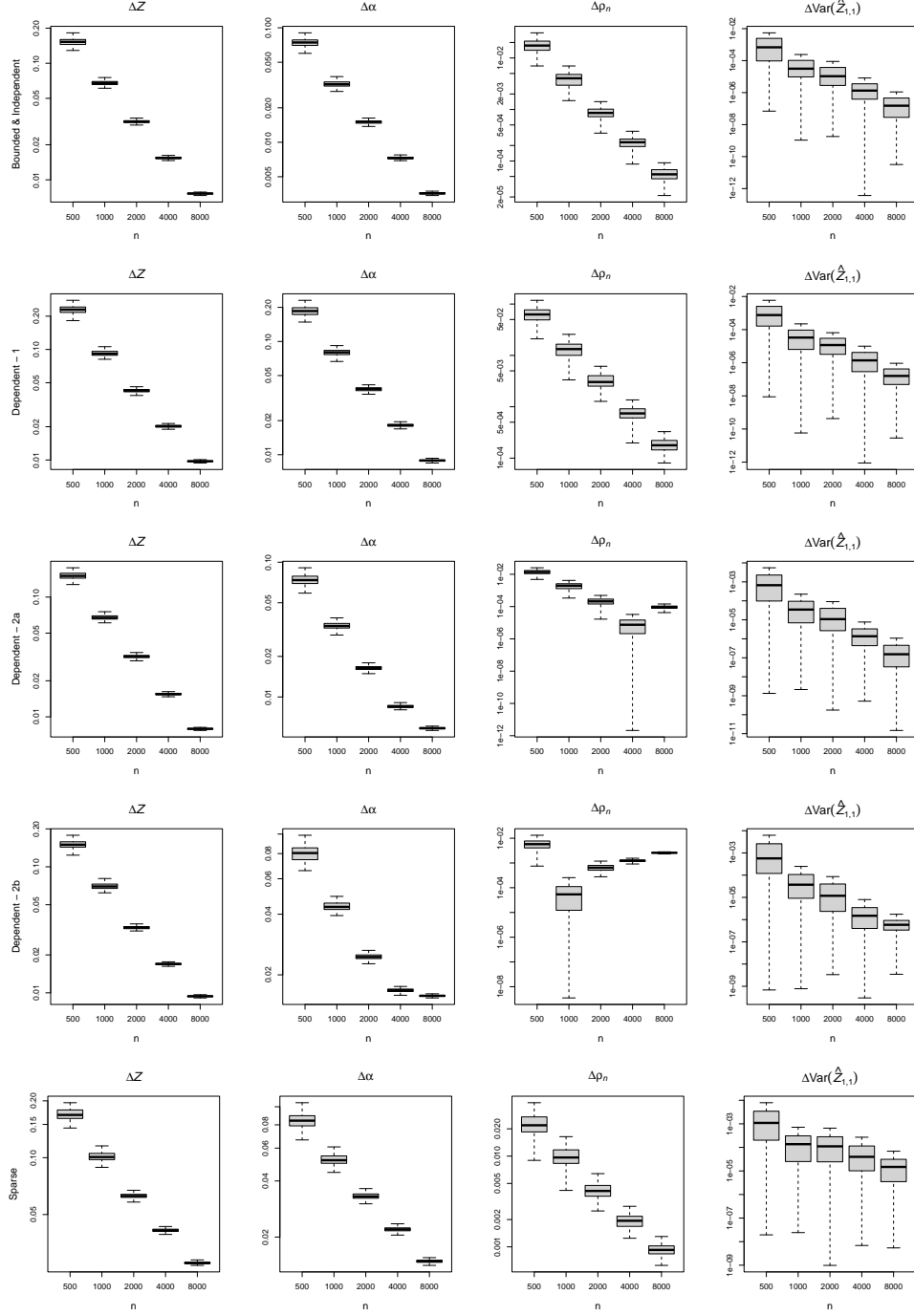


FIG 1. Consistency plots for maximum likelihood estimators under different settings.

et al., 2021], where the correlation between nodes i and j are defined by $\prod_{l=i-1}^j \rho_l$ and ρ_l are determined by the marginal probabilities θ_{ij} . The consistency plots are illustrated in the second row of Figure 1 and the coverage results are reported in the second rows of Table 1 and Table 2. The histograms and QQ-plots are illustrated in the first two rows of Figure 3. We can see that the theoretical results remain valid under this dependent setting.

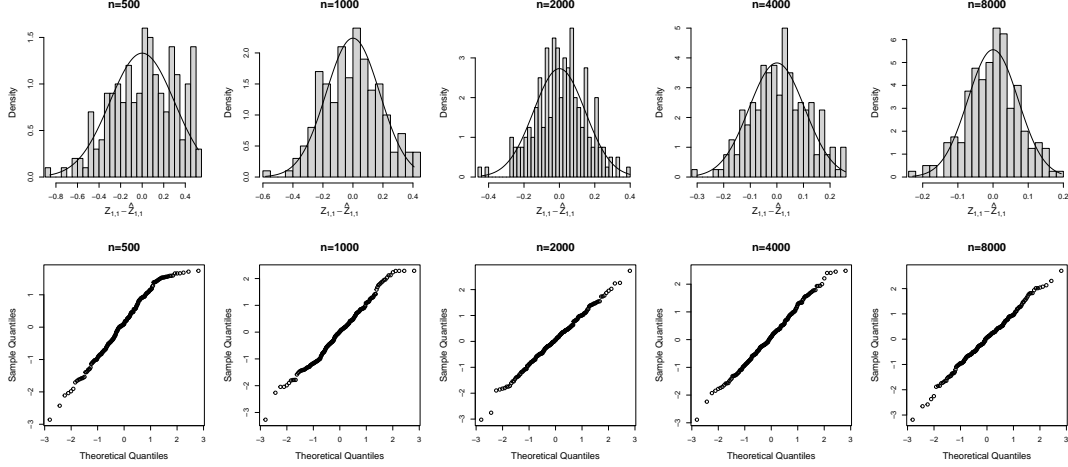


FIG 2. Empirical versus theoretical distribution plots under the “Bounded & Indep.” setting.

Setting	Coverage of z_{11}				
Bounded & Indep.	0.970 (0.0121)	0.940 (0.0168)	0.960 (0.0139)	0.955 (0.0147)	0.930 (0.0180)
Dependent-1	0.970 (0.0121)	0.915 (0.0197)	0.935 (0.0174)	0.945 (0.0161)	0.955 (0.0147)
Dependent-2a	0.975 (0.0110)	0.930 (0.0180)	0.960 (0.0139)	0.955 (0.0147)	0.935 (0.0174)
Dependent-2b	0.970 (0.0121)	0.940 (0.0168)	0.965 (0.0130)	0.955 (0.0147)	0.965 (0.0130)
Sparse	0.975 (0.0110)	0.930 (0.0180)	0.940 (0.0168)	0.945 (0.0161)	0.930 (0.0180)
n	500	1000	2000	4000	8000

TABLE 1

Coverage rates of 95% confidence intervals for z_{11} with standard deviation under different settings.

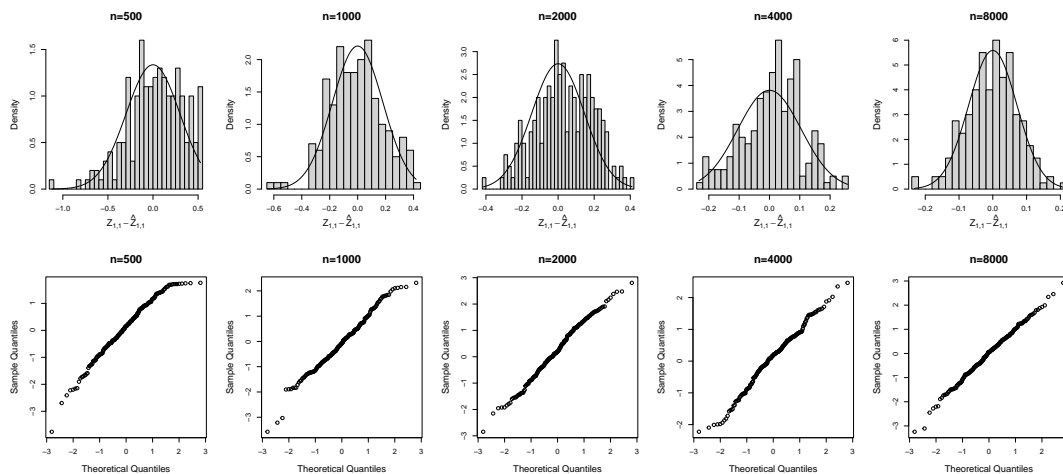
Setting	Coverage of θ_{12}				
Bounded & Indep.	0.890 (0.0221)	0.940 (0.0168)	0.955 (0.0147)	0.925 (0.0186)	0.935 (0.0174)
Dependent-1	0.905 (0.0207)	0.925 (0.0186)	0.875 (0.0234)	0.925 (0.0186)	0.940 (0.0168)
Dependent-2a	0.885 (0.0226)	0.940 (0.0168)	0.950 (0.0154)	0.925 (0.0186)	0.940 (0.0168)
Dependent-2b	0.885 (0.0226)	0.960 (0.0139)	0.930 (0.0180)	0.865 (0.0242)	0.000 (0.0000)
Sparse	0.875 (0.0234)	0.930 (0.0180)	0.940 (0.0168)	0.935 (0.0174)	0.960 (0.0139)
n	500	1000	2000	4000	8000

TABLE 2

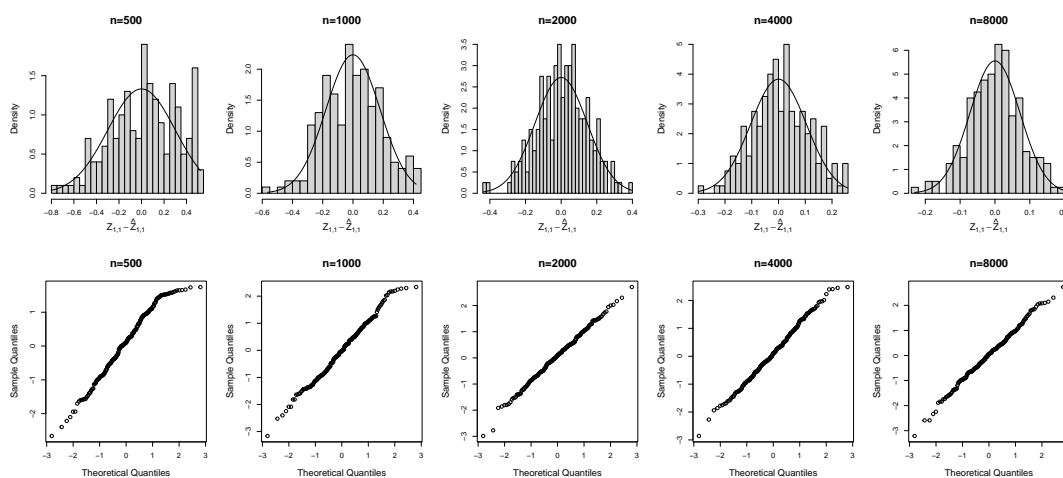
Coverage rates of 95% confidence intervals for θ_{12} with standard deviation under different settings. The dashed red line is the theoretical value of 0.95.

The second setting being considered is to introduce dependency with an additional dimension of latent position that occurs in the data generating process while being ignored in model fitting. In addition to the generating process of Z , α , and ρ_n as before, we further generate 1-dimensional positions with Hadamard product $Z_{dep} \odot E$, where entries $Z_{dep} \stackrel{i.i.d.}{\sim} \mathcal{N}_{[-2,2]}(0,1)$ and E is an indicator vector with a certain proportion of random entries to be 1 and the rest being 0. The Z_{dep} will only appear in data generation while not being estimated during model fitting, thus introducing implicit edge dependency. The non-zero proportions are set to be 25% and 50%, referred as “Dependent-2a” and “Dependent-2b” settings, respectively. Note that here we deliberately select relatively strong dependent cases with non-zero proportions 25% and 50% to give a full illustration of the strengths and the limitations of our theoretical results.

Histograms and QQ-plots under Dependent-1



Histograms and QQ-plots under Dependent-2a



Histograms and QQ-plots under Dependent-2b

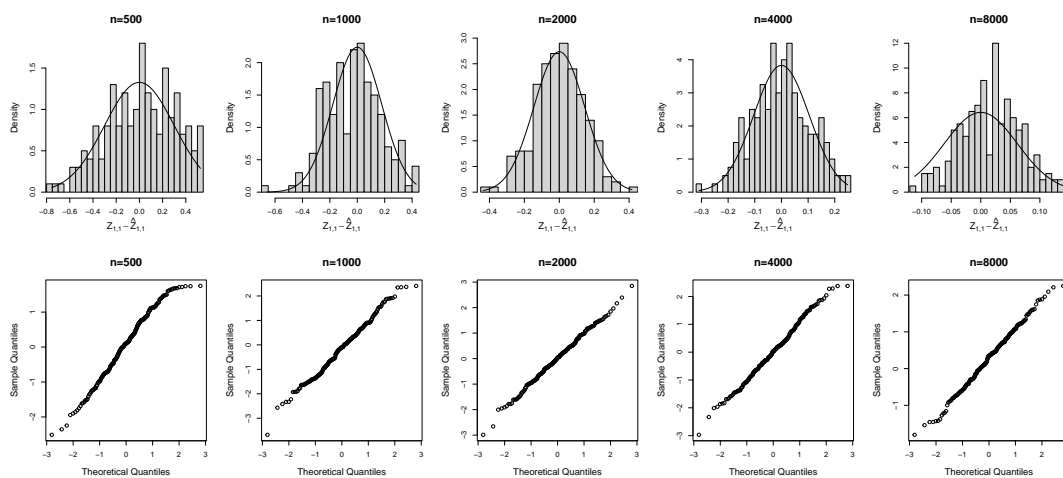


FIG 3. Empirical versus theoretical distribution plots under the dependent settings: "Dependent-1", "Dependent-2a", and "Dependent-2b".

The consistency plots are illustrated in the third and fourth rows of Figure 1, the average coverage rates are reported in Table 1 and Table 2, and the corresponding histograms and QQ-plots for “Dependent-2a” and “Dependent-2b” settings are presented in Figure 3. From Figure 3 and Table 1, we can see that the individual asymptotic approximation still performs well. On the other hand, it is interesting to observe from Figure 1 that $\hat{\alpha}$ and $\hat{\rho}_n$ are no longer showing ideal consistency patterns. Note that the scale of $\Delta\rho_n$ is much smaller than $\Delta\alpha$, and our theory focuses only on α . Thus, the most serious deviation of the experiment result happens when $n = 8000$ under the “Dependent-2b” setting. To explain this observation, we check the validity of Assumption IX and summarize the average values of $\|S(\hat{\phi})\|$ of “Dependent-1”, “Dependent-2a”, and “Dependent-2b” with different values of n in the supplementary materials. Under Assumption IX, the norm of the score vector should not increase significantly as n increases. However, we find that $\|S(\hat{\phi})\| = 0.53$ when $n = 8000$ under the “Dependent-2b” setting, whereas the values are around 0.13 for the rest situations. This indicates under the “Dependent-2b” setting, the dependency of edges might be too strong, and as a consequence the assumptions required for the validity of the theorems no longer hold. Interestingly, the coverage rates reported in the third and fourth rows of Table 1 and Table 2 show consistent patterns. While most of the entries are around 0.95 as n grows, when $n = 8000$ under the “Dependent-2b” setting, the estimated variance of $\hat{\theta}_{1,2}$ is significantly smaller than the theoretical value due to the strong dependency, resulting in zero coverage.

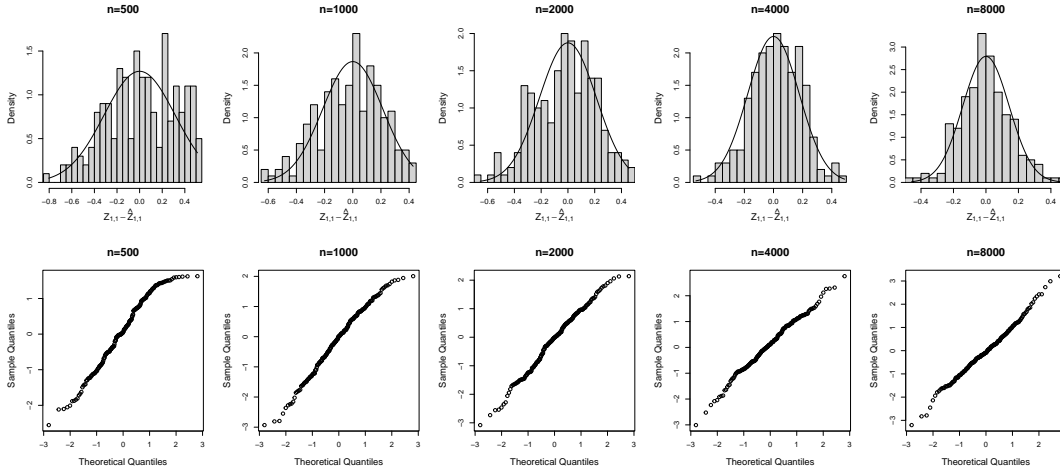


FIG 4. Empirical versus theoretical distribution plots under the “Sparse” setting.

4.4. Sparse Networks. In the sparse edge setting, referred to as “Sparse”, we generate Z and α following the same way as in Section 4.2 while setting $\rho_n = -\frac{1}{2} \log n$, which is on the borderline of violating Assumption I*. Under this construction, the average edge density of generated networks decreases from 0.07 to 0.02 as n increases from 500 to 8000. The consistency plots are illustrated in the last row of Figure 1, where we can see that the consistency rates is related to ρ_n and meet the theoretical value of $O_p(\frac{1}{w_n n}) = O_p(\frac{1}{\sqrt{n}})$. The coverage rates are reported in the fifth rows of Table 1 and Table 2, showing that the empirical values meet the expectation well as n grows. The histograms and QQ-plots for the distribution of latent position estimators are illustrated in Figure 4. These results demonstrate that our theory remains valid in the sparse edge setting.

5. Analysis of The Statistician Coauthorship Network. We demonstrate the usefulness of our statistical inference results via an application to a statistician coauthorship network. The data is collected by the authors of [Ji and Jin \[2016\]](#), consisting of authorship information of papers published in four of the top statistical journals from 2003 to 2012. In this coauthorship network, each node represents a statistician, and two statisticians are connected if they have coauthored at least 2 papers. Our analysis focuses on the largest connected component, with $n = 236$ statisticians and 296 edges. Consistently with [Ji and Jin \[2016\]](#), we use the scree-plot and choose to fit a two-dimensional latent space model on the coauthorship network.

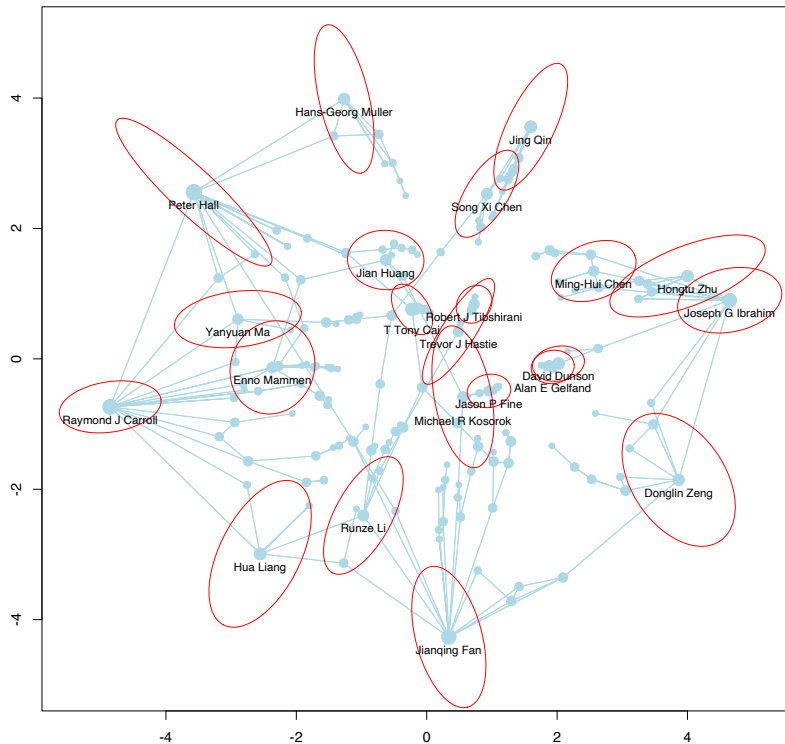


FIG 5. The estimated latent positions with 95% confidence regions of hub nodes. Nodes are scaled by degrees.

The estimated latent positions are visualized in Figure 5, providing insights into the collaboration patterns and research interests of statisticians within the network. The node sizes are proportional to the node degrees, with larger nodes representing higher degrees. We highlight those hub nodes (node degrees greater than 5) with the corresponding statisticians' names for better interpretation. A direct examination of the point estimates shows that the estimated two-dimensional latent positions uncover certain community structures among statisticians, which include groups such as non-parametric and semi-parametric (left), high-dimensional statistics (bottom), Bayesian statistics and Biostatistics (right), and statistical learning (middle). These observations align with the findings from related studies [\[Ji and Jin, 2016\]](#). However, our inference theories enable us to investigate beyond point estimation. We can construct confidence regions for the estimated latent positions, offering deeper insights into the

network’s nuances. In Figure 5, 95% confidence regions for the latent positions of the hub nodes are indicated by the red elliptical contours.

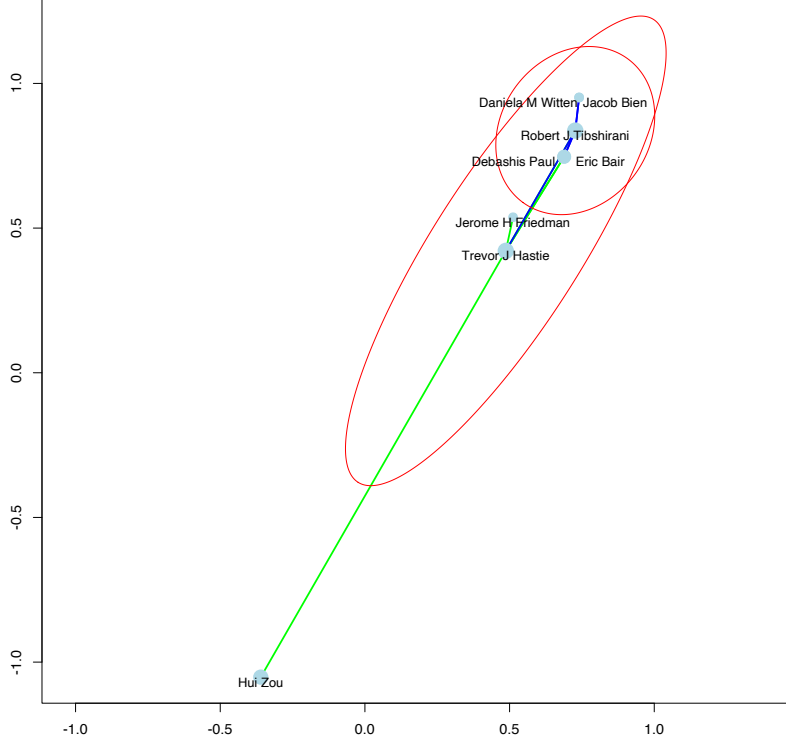


FIG 6. An example involving two statisticians, Robert J Tibshirani and Trevor J Hastie, with their collaborators. The blue and green lines are collaborations of Trevor J Hastie and Robert J Tibshirani, respectively. The 95% confidence regions of the two statisticians are plotted in red.

We further provide a statistical interpretation of the elliptical confidence regions about their sizes, shapes, and orientations. Based on Equations (6) and (10), the influential terms in the variance of the latent position estimator are those contributed by their neighboring nodes. In particular, the sizes of ellipses diminish with an increase in node degrees but expand with greater variance of the latent positions of their neighboring nodes. Thus, the estimation uncertainty of statisticians’ latent positions decreases with the number of collaborators while increasing with greater cross-domain collaborations. Also by Equations (6) and (10), the orientations of the ellipses’ major and minor axes are largely influenced by the collaborators’ latent positions. Additionally, the extend of overlap between ellipses can shed light on the similarity in collaboration patterns or research interests between statisticians.

To further illustrate this, Figure 6 shows an example involving two statisticians, Dr. Robert J. Tibshirani and Dr. Trevor J. Hastie, and their collaborators. While in this network, these two nodes have the same degrees and the latent positions are relatively close to each other, their ellipses have quite different sizes and orientations. Such a difference is primarily influenced by the estimated latent positions of collaborators in this network, as indicated in the figure.

6. Discussion. In this paper, we address the crucial statistical inference problems of the latent space models for network data. Adopting a flexible analysis framework utilizing the Lagrange-adjusted Hessian matrix, which has not been introduced in the existing network literature, we prove the first uniform consistency and asymptotic distribution results for maximum likelihood estimators in a broad class of latent space models, accommodating different edge types and link functions. Furthermore, extensions have been established for two realistic yet challenging scenarios concerning edge dependency and sparsity. We conduct extensive simulation studies to validate the theoretical results and provide a data application focused on a statistician coauthorship network, demonstrating how the established theories can provide valuable insights into network structure beyond point estimation.

Our analysis techniques point to several promising future directions for downstream inference problems beyond link prediction. The first direction involves network testing and node testing problems. Multi-network comparisons have been recently studied in the RDGP literature [Athreya et al., 2017], and two sample tests of a set of nodes have been studied in neuroimaging applications [Li et al., 2018]. Our theoretical results can potentially be utilized to develop similar tests for a wide range of network data. The second direction concerns complex data with node covariates along with network edges. Our theories can be employed to conduct statistical inference for network-assisted prediction by considering the estimation uncertainty of latent positions, where the estimated network latent positions are used to facilitate prediction along with node covariates [Lunde et al., 2023, Zhang et al., 2022].

SUPPLEMENTARY MATERIAL

Supplement to “Statistical Inference on Latent Space Models for Network Data”

The supplementary material contains additional simulation results and the proofs of main results.

REFERENCES

- John Aitchison and SD Silvey. Maximum-likelihood estimation of parameters subject to restraints. *The annals of mathematical Statistics*, 29(3):813–828, 1958.
- Enrico Amico and Joaquín Goñi. Mapping hybrid functional-structural connectivity traits in the human connectome. *Network Neuroscience*, 2(3):306–322, 2018.
- Avanti Athreya, Donniell E Fishkind, Minh Tang, Carey E Priebe, Youngser Park, Joshua T Vogelstein, Keith Levin, Vince Lyzinski, and Yichen Qin. Statistical inference on random dot product graphs: a survey. *The Journal of Machine Learning Research*, 18(1):8393–8484, 2017.
- Jushan Bai. Inferential theory for factor models of large dimensions. *Econometrica*, 71(1):135–171, 2003.
- Jushan Bai and Yuan Liao. Statistical inferences using large estimated covariances for panel data and factor models. *arXiv preprint arXiv:1307.2662*, 2013.
- Ed Bullmore and Olaf Sporns. Complex brain networks: graph theoretical analysis of structural and functional systems. *Nature Reviews Neuroscience*, 10(3):186–198, 2009.
- Joshua Cape, Minh Tang, and Carey E Priebe. Signal-plus-noise matrix models: eigenvector deviations and fluctuations. *Biometrika*, 106(1):243–250, 2019.
- Thomas Chaney. The network structure of international trade. *American Economic Review*, 104(11):3600–3634, 2014.
- Harini Eavani, Theodore D Satterthwaite, Roman Filipovych, Raquel E Gur, Ruben C Gur, and Christos Davatzikos. Identifying sparse connectivity patterns in the brain using resting-state fmri. *Neuroimage*, 105: 286–299, 2015.
- Abdalla T El-Helbawy and Tawfik Hassan. On the wald, lagrangian multiplier and likelihood ratio tests when the information matrix is singular. *Journal of The Italian Statistical Society*, 3:51–60, 1994.
- Peter D Hoff, Adrian E Raftery, and Mark S Handcock. Latent space approaches to social network analysis. *Journal of the american Statistical association*, 97(460):1090–1098, 2002.
- Paul W Holland, Kathryn Blackmond Laskey, and Samuel Leinhardt. Stochastic blockmodels: First steps. *Social networks*, 5(2):109–137, 1983.

- Pengsheng Ji and Jiashun Jin. Coauthorship and citation networks for statisticians. *The Annals of Applied Statistics*, 10(4):1779–1812, 2016.
- Wei Jiang, Shuang Song, Lin Hou, and Hongyu Zhao. A set of efficient methods to generate high-dimensional binary data with specified correlation structures. *The American Statistician*, 75(3):310–322, 2021.
- Lexin Li, Jian Kang, Samuel N Lockhart, Jenna Adams, and William J Jagust. Spatially adaptive varying correlation analysis for multimodal neuroimaging data. *IEEE transactions on medical imaging*, 38(1):113–123, 2018.
- Robert Lunde, Elizaveta Levina, and Ji Zhu. Conformal prediction for network-assisted regression. *arXiv preprint arXiv:2302.10095*, 2023.
- Zhuang Ma, Zongming Ma, and Hongsong Yuan. Universal latent space model fitting for large networks with edge covariates. *Journal of Machine Learning Research*, 21:4–1, 2020.
- Samuel D Silvey. The lagrangian multiplier test. *The Annals of Mathematical Statistics*, 30(2):389–407, 1959.
- Anna L Smith, Dena M Asta, and Catherine A Calder. The geometry of continuous latent space models for network data. *Statistical Science*, 34(3):428, 2019.
- Will Wei Sun and Lexin Li. Store: sparse tensor response regression and neuroimaging analysis. *The Journal of Machine Learning Research*, 18(1):4908–4944, 2017.
- Amanda L Traud, Peter J Mucha, and Mason A Porter. Social structure of facebook networks. *Physica A: Statistical Mechanics and its Applications*, 391(16):4165–4180, 2012.
- Fa Wang. Maximum likelihood estimation and inference for high dimensional generalized factor models with application to factor-augmented regressions. *Journal of Econometrics*, 229(1):180–200, 2022.
- Yikai Wang and Ying Guo. Locus: A regularized blind source separation method with low-rank structure for investigating brain connectivity. *The Annals of Applied Statistics*, 17(2):1307–1332, 2023.
- Stephen J Young and Edward R Scheinerman. Random dot product graph models for social networks. In *International Workshop on Algorithms and Models for the Web-Graph*, pages 138–149. Springer, 2007.
- Xuefei Zhang, Gongjun Xu, and Ji Zhu. Joint latent space models for network data with high-dimensional node variables. *Biometrika*, 109(3):707–720, 2022.
- Yunpeng Zhao, Elizaveta Levina, and Ji Zhu. Consistency of community detection in networks under degree-corrected stochastic block models. *The Annals of Statistics*, 2012.